

Pre-Treatment Clinical and Biochemical Predictors of Therapy Response in Differentiated Thyroid Cancer Using Random Forest Models

Jun Costa¹, Jun Zhang¹, Emily M. Lopez^{1*}, Ingrid Singh¹, Ayesha Moore¹

¹Department of Clinical Cancer Research, School of Medicine, Sapienza University of Rome, Rome, Italy.

*E-mail  elopez@outlook.com

Received: 14 January 2023; Revised: 22 March 2023; Accepted: 25 March 2023

ABSTRACT

The goal of this study was to construct a machine-learning framework to forecast patient response to radioiodine (131I) treatment and thyrotropin (TSH) suppression treatment in individuals with differentiated thyroid cancer (DTC) lacking structural evidence of disease, using only data available before treatment. In total, 597 patients were randomly selected for the training set to predict response to 131I therapy, while 326 were assigned for predicting response to TSH suppression therapy, all with DTC and no structural disease. Six different supervised machine-learning techniques were applied: Logistic Regression, Support Vector Machine, Random Forest (RF), Neural Networks, Adaptive Boosting, and Gradient Boost. These models were trained to identify effective response (ER) to 131I therapy and biochemical remission (BR) to TSH suppression therapy. The key predictors of ER to 131I therapy were pre-treatment stimulated and suppressed thyroglobulin (Tg) values as well as radioiodine uptake before the ongoing 131I course. For Tg reduction during TSH suppression therapy, the main contributors were visible thyroid remnant on the post-treatment whole-body scan from the previous 131I course and TSH values. Random Forest (RF) outperformed the other algorithms. Using RF, the accuracy and area under the receiver operating characteristic curve (AUC) for differentiating ER from non-ER in 131I therapy reached 81.3% and 0.896, respectively. For forecasting BR during TSH suppression therapy, RF achieved an accuracy of 78.7% and an AUC of 0.857. These findings highlight the value of machine-learning approaches, particularly the Random Forest algorithm, as effective instruments for anticipating response to 131I therapy and TSH suppression therapy in DTC patients without structural disease, drawing solely on standard pre-treatment clinical parameters and laboratory indicators.

Keywords: DTC without structural disease, 131I therapy, TSH suppression therapy, Thyroglobulin, Random forest

How to Cite This Article: Costa J, Zhang J, Lopez EM, Singh I, Moore A. Pre-Treatment Clinical and Biochemical Predictors of Therapy Response in Differentiated Thyroid Cancer Using Random Forest Models. *Asian J Curr Res Clin Cancer*. 2023;3(2):121-34. <https://doi.org/10.51847/PINHGUhQWn>

Introduction

Differentiated thyroid cancer (DTC) constitutes the majority of thyroid malignancies, representing roughly 90% of cases [1]. With the rise in routine medical check-ups, most DTC diagnoses now occur early, commonly showing no imaging signs of ongoing disease after complete thyroid removal [2]. Typical management includes surgery, radioiodine (131I) therapy, and TSH suppression therapy. The purpose of post-operative 131I therapy is to eliminate any remaining normal thyroid tissue and to address possible undetected residual cancer or biochemical signs of persistence [3, 4]. Patients require levothyroxine (LT4) both to replace missing thyroid hormone and to prevent tumor progression [5]. American Thyroid Association (ATA) guidelines recommend a risk-adapted strategy for TSH suppression to balance benefits against risks of over-suppression [6].

Monitoring thyroglobulin (Tg) is standard for evaluating therapy success and detecting potential recurrence or spread after thyroidectomy and 131I treatment [7-10]. Both stimulated (Tgoff) and suppressed (Tgon) Tg measurements are vital for overseeing DTC patients without visible structural disease [11]. Low post-ablation Tg suggests no remaining active cancer, permitting longer follow-up intervals of 12-24 months [3]. In contrast,

persistently high or increasing Tg may prompt further investigations, and even without structural findings, additional treatment could be considered to lower recurrence risk [12]. Reaching the lowest Tg level allows downward adjustment of recurrence risk and possible re-stratification to very low risk [13].

While ^{131}I therapy and TSH suppression are both viewed as useful for keeping Tg under control in DTC patients without structural disease [14, 15], the degree of Tg reduction they produce remains debated [3, 16, 17]. Selecting patients who will truly benefit from these interventions is therefore essential. Earlier research identified predictors of response mainly via standard univariate and multivariate statistics, but these methods struggle with intricate inter-variable relationships [18], limiting pre-treatment prediction accuracy until now.

Machine-learning methods excel at discovering hidden patterns in historical data and handling complicated interactions among many variables [19]. Such models can reveal deeper connections between predictors and outcomes, especially with interacting factors. We thus examined a substantial group of DTC patients without structural disease who received ^{131}I therapy, followed by TSH suppression and extended follow-up at one institution. Our aim was to build and assess an artificial intelligence tool to anticipate response to ^{131}I therapy and subsequent TSH suppression therapy, incorporating routinely gathered pre-treatment variables linked to treatment success to support clinical decisions.

Materials and Methods

Study populations

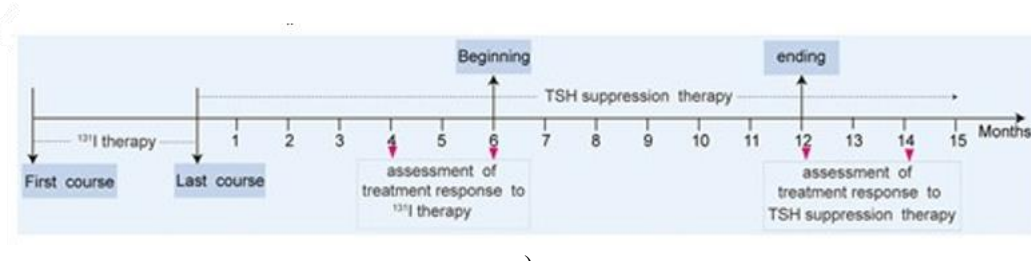
This retrospective study included adult patients (>18 years) with differentiated thyroid cancer (DTC) and no structural disease who had total or near-total thyroidectomy plus cervical lymph node dissection at our center between January 2011 and December 2020. Eligible participants met these conditions: (1) completion of at least one ^{131}I treatment cycle; (2) availability of pre-current-cycle tests including TSH, Tg, TgAb, RAIU%, neck ultrasound, and chest CT, plus repeat assessments 4-6 months and 12-14 months after the prior cycle. Cases were excluded if patients (1) already had undetectable suppressed Tg ($\text{Tg}_{\text{on}} < 0.2 \text{ ng/mL}$) pre-therapy, (2) developed lymph node or distant metastases within 6 months post-therapy, or (3) lacked complete follow-up records. Ethical approval was granted by the Ethics Committee of the First Hospital of Jilin University.

Every ^{131}I treatment cycle consisted of oral dosing with 1.85-3.70 GBq (50-100 mCi). A post-therapy whole-body scan (Rx-WBS) using SPECT/CT was obtained three days later. Levothyroxine (LT4) dose modifications, when required, occurred 1-6 months after treatment. Response evaluation for ^{131}I therapy took place 4-6 months following the final cycle.

Candidate predictors of ^{131}I therapy response comprised: age, gender, histologic type, TNM-T, TNM-N, stage, risk category, pre-withdrawal TSH (TSH_{on}), suppressed Tg (Tg_{on}), pre-withdrawal TgAb (TgAb_{on}), post-withdrawal TSH at 4 weeks (TSH_{off}), stimulated Tg (Tg_{off}), post-withdrawal TgAb at 4 weeks (TgAb_{off}), RAIU% prior to the current cycle, and previous ^{131}I cycle count. For TSH suppression response, evaluated variables were: age, gender, histologic type, TNM-T, TNM-N, stage, risk category, RAIU% before the final cycle, total cycle count, remnant thyroid visibility on Rx-WBS after the final cycle, TSH, suppressed Tg, and TgAb measured 4-6 months post-final cycle (TSH_{six}, Tg_{six}, TgAb_{six}).

Treatment response to ^{131}I therapy

Response classification for ^{131}I therapy followed slightly modified ATA criteria and was performed 4-6 months after the last cycle (**Figure 1a**). Effective response (ER) required undetectable suppressed Tg ($< 0.2 \text{ ng/mL}$). Non-ER included detectable suppressed Tg ($\geq 0.2 \text{ ng/mL}$) or rising pre-withdrawal TgAb.



a)

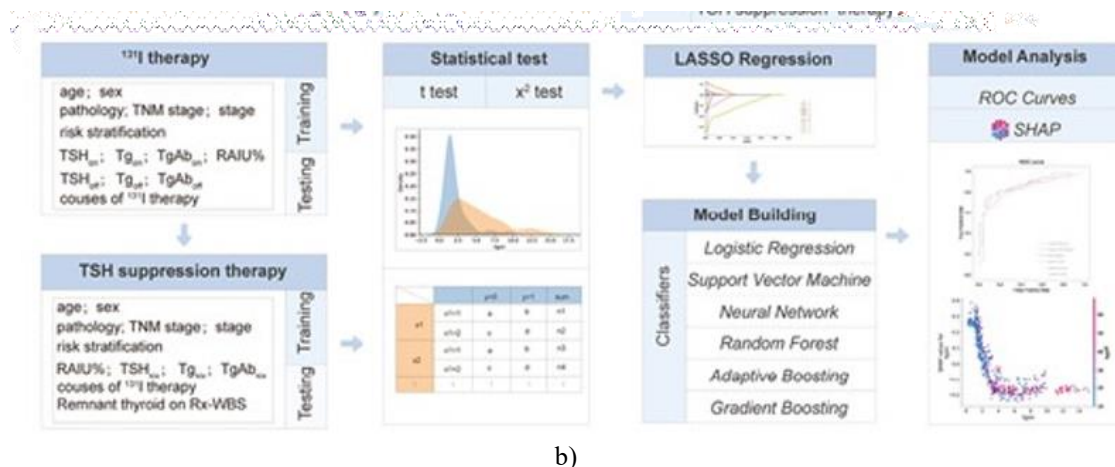


Figure 1. Workflow for predicting treatment response to radioiodine (131I) therapy and thyrotropin (TSH) suppression therapy in differentiated thyroid cancer patients without structural disease. (a) The time point of treatment response assessment in 131I therapy and TSH suppression therapy. (b) Workflow for establishment and validation of predicting models with different algorithms.

Treatment response to TSH suppression therapy

Response to TSH suppression was quantified via the percentage change in suppressed Tg ($\Delta T_{\text{gon}}\%$), comparing levels at 6 months (pre-suppression) versus 12–14 months (post-suppression) after the last 131I cycle (**Figure 1a**). The formula used was: (pre-suppression Tgon – post-suppression Tgon) / pre-suppression Tgon \times 100%. Biochemical remission (BR) was assigned when $\Delta T_{\text{gon}}\% \geq 25.0\%$ (indicating $\geq 25.0\%$ Tg drop), while non-BR applied when $\Delta T_{\text{gon}}\% < 25.0\%$ (covering any Tg rise or drop $< 25.0\%$).

Establishment and evaluation of machine learning algorithms

The study process is outlined in **Figure 1b**. Predictive modeling was patient-specific. Enrolled cases were repeatedly randomized (10-fold cross-validation) into training (70%) and testing (30%) sets. Initial screening compared groups using Wilcoxon tests for continuous data and Chi-square/Fisher's exact tests for categorical data. Significant variables ($P < .05$) then underwent feature reduction by LASSO regression with 10-fold cross-validation. Selected features fed into model training using six algorithms: Logistic Regression (LG), Support Vector Machine (SVM), Random Forest (RF), Neural Networks (NN), Adaptive Boosting (ADA), and Gradient Boost (GB).

Feature importance and directional effects were interpreted via SHapley Additive exPlanations (SHAP) summary plots. For 131I response, “0” coded ER and “1” coded non-ER; higher positive SHAP scores raised non-ER probability, lower negative scores favored ER. For TSH suppression, “0” coded BR and “1” coded non-BR; positive SHAP increased non-BR likelihood, negative SHAP favored BR. These plots visually ranked influential predictors and clarified their impact on outputs.

All models were benchmarked primarily through receiver operating characteristic (ROC) curves and area under the curve (AUC) values derived from the testing set.

Results and Discussion

Patient characteristics for predicting treatment response to 131I Therapy

For the training set, 843 patients without structural disease were initially considered. After removing 246 individuals (89 due to undetectable Tgon, 56 who showed structural disease within 6 months post-131I therapy, and 101 owing to incomplete follow-up), 70.8% (597/843) qualified for inclusion. The testing set started with 339 patients without structural disease. Following removal of 82 cases (32 with undetectable Tgon, 8 who developed structural disease within 6 months after therapy, and 42 with missing follow-up data), 75.8% (257/339) were retained. **Table 1** confirms that no variables differed significantly between the training and testing groups.

Table 1. Baseline characteristics of differentiated thyroid cancer patients without structural disease in the training and testing cohorts for prediction of treatment response to 131I therapy (N = 854).

Feature	Testing Group (n = 257)	Training Group (n = 597)	P-value
Gender			.25
Female	173 (67.3%)	426 (71.4%)	
Male	84 (32.7%)	171 (28.6%)	
Age, median (years)	43 (IQR, 33~53)	45 (IQR, 36~54)	.12
Histology			1.00
Papillary thyroid carcinoma	253 (98.4%)	586 (98.2%)	
Follicular thyroid carcinoma	4 (1.6%)	11 (1.8%)	
TNM-T stage			.55
T1	167 (65.0%)	397 (66.5%)	
T2	52 (20.3%)	98 (16.4%)	
T3	24 (9.3%)	66 (11.1%)	
T4	14 (5.4%)	36 (6.0%)	
TNM-N stage			.16
N0	14 (5.4%)	48 (8.1%)	
N1a	108 (42.0%)	215 (36.0%)	
N1b	135 (52.6%)	334 (55.9%)	
Clinical stage			.78
I	208 (80.9%)	471 (78.9%)	
II	48 (18.7%)	122 (20.4%)	
III	1 (0.4%)	4 (0.7%)	
IV	0 (0%)	0 (0%)	
Risk category			.87
Low	25 (9.7%)	60 (10.1%)	
Intermediate	206 (80.2%)	483 (80.9%)	
High	26 (10.1%)	54 (9.0%)	
RAIU%, median	6.0 (IQR, 3.7~8.5)	6.5 (IQR, 4.2~8.6)	.12
TSHon, median (mIU/L)	0.25 (IQR, 0.07~0.68)	0.32 (IQR, 0.08~0.75)	.16
Tgon, median (ng/mL)	2.61 (IQR, 1.46~4.65)	2.68 (IQR, 1.52~5.43)	.25
TgAbon, median (IU/mL)	11.20 (IQR, 10.00~15.92)	11.70 (IQR, 10.00~17.09)	.42
TSHoff, median (mIU/L)	100.00 (IQR, 95.40~100.00)	100.00 (IQR, 95.20~100.00)	.23
Tgoff, median (ng/mL)	21.39 (IQR, 14.07~36.24)	22.09 (IQR, 15.37~36.75)	.18
TgAboff, median (IU/mL)	12.00 (IQR, 10.00~16.92)	11.87 (IQR, 10.00~17.80)	.94
Number of 131I courses			.94
0	178 (69.3%)	411 (68.8%)	
≥1	79 (30.7%)	186 (31.2%)	

Abbreviations: PTC, papillary thyroid cancer; FTC, follicular thyroid cancer; TSHon, thyroid-stimulating hormone before Levothyroxine withdrawal; Tgon, suppressed thyroglobulin; TgAbon, antithyroglobulin antibody before Levothyroxine withdrawal; TSHoff, thyroid-stimulating hormone after Levothyroxine withdrawal; Tgoff, stimulated thyroglobulin; TgAboff, antithyroglobulin antibody after Levothyroxine withdrawal; IQR, interquartile range; RAIU, radioiodine uptake.

Predicting treatment response to 131I Therapy

Within the training group, 45.2% (270/597) of cases attained ER following 131I therapy, compared to 54.8% (327/597) exhibiting non-ER (**Table 2**). Corresponding figures in the testing group were 45.5% (117/257) for ER and 54.5% (140/257) for non-ER.

Table 2. Comparison of clinical characteristics of differentiated thyroid cancer patients without structural disease who obtained ER or non-ER to 131I therapy in the training and testing cohorts (N = 854).

Feature	Testing Group		Training Group		P-value
	ER (n = 117)	Non-ER (n = 140)	ER (n = 270)	Non-ER (n = 327)	
Gender			.18		.03
Female	84 (71.8%)	89 (63.6%)	205 (75.9%)	221 (67.6%)	
Male	33 (28.2%)	51 (36.4%)	65 (24.1%)	106 (32.4%)	

Age, median (years)	44 (IQR, 35-55)	42 (IQR, 32-52)	.07	45 (IQR, 36-53)	45 (IQR, 36-54)	.69
Histology			.13			1.00
Papillary thyroid carcinoma	117 (100.0%)	136 (97.1%)		265 (98.1%)	321 (98.2%)	
Follicular thyroid carcinoma	0 (0.0%)	4 (2.9%)		5 (1.9%)	6 (1.8%)	
TNM-T stage			.64			.69
T1	77 (65.8%)	90 (64.3%)		184 (68.1%)	213 (65.1%)	
T2	25 (21.4%)	27 (19.3%)		39 (14.4%)	59 (18.0%)	
T3	8 (6.8%)	16 (11.4%)		30 (11.1%)	36 (11.0%)	
T4	7 (6.0%)	7 (5.0%)		17 (6.3%)	19 (5.8%)	
TNM-N stage			.46			.01
N0	8 (6.8%)	6 (4.3%)		24 (8.9%)	24 (7.3%)	
N1a	52 (44.4%)	56 (40.0%)		116 (43.0%)	99 (30.3%)	
N1b	57 (48.8%)	78 (55.7%)		130 (48.1%)	204 (62.4%)	
Clinical stage			.09			.69
I	89 (76.0%)	119 (85.0%)		216 (80.0%)	255 (78.0%)	
II	27 (23.1%)	21 (15.0%)		53 (19.6%)	69 (21.1%)	
III	1 (0.9%)	0 (0%)		1 (0.4%)	3 (0.9%)	
IV	0 (0%)	0 (0%)		0 (0%)	0 (0%)	
Risk category			.01			.01
Low	16 (13.6%)	9 (6.4%)		36 (13.3%)	24 (7.3%)	
Intermediate	96 (82.1%)	110 (78.6%)		224 (83.0%)	259 (79.2%)	
High	5 (4.3%)	21 (15.0%)		10 (3.7%)	44 (13.5%)	
RAIU%, median	5.9 (IQR, 3.8-8.4)	6.0 (IQR, 3.7-8.7)	.96	6.9 (IQR, 4.9-8.7)	6.1 (IQR, 3.5-8.5)	.01
TSH_{on}, median (mIU/L)	0.22 (IQR, 0.07-0.57)	0.28 (IQR, 0.08-0.71)	.14	0.39 (IQR, 0.09-0.83)	0.27 (IQR, 0.07-0.70)	.03
T_gon, median (ng/mL)	1.43 (IQR, 1.16-2.23)	4.32 (IQR, 2.51-6.51)	.01	1.60 (IQR, 1.24-2.44)	4.39 (IQR, 2.52-7.07)	.01
T_gAbon, median (IU/mL)	11.6 (IQR, 10.00-16.09)	10.71 (IQR, 10.00-15.65)	.13	11.62 (IQR, 10.00-17.31)	11.73 (IQR, 10.00-17.05)	.87
TSH_{off}, median (mIU/L)	100.00 (IQR, 92.70-100.00)	100.00 (IQR, 96.66-100.00)	.58	100.00 (IQR, 97.70-100.00)	100.00 (IQR, 88.10-100.00)	.13
T_goff, median (ng/mL)	15.10 (IQR, 11.97-19.67)	31.89 (IQR, 20.29-42.98)	.01	16.37 (IQR, 12.00-22.60)	30.83 (IQR, 21.00-47.00)	.01
T_gAboff, median (IU/mL)	11.50 (IQR, 10.00-15.69)	12.70 (IQR, 10.00-17.39)	.14	11.43 (IQR, 10.00-16.70)	12.00 (IQR, 10.00-18.20)	.27
Number of 131I courses			.01			.01
0	96 (82.1%)	82 (58.6%)		221 (81.9%)	190 (58.1%)	
≥1	21 (17.9%)	58 (41.4%)		49 (18.1%)	137 (41.9%)	

Abbreviations: ER, excellent response; PTC, papillary thyroid cancer; FTC, follicular thyroid cancer; TSH_{on}, thyroid-stimulating hormone before Levothyroxine withdrawal; T_gon, suppressed thyroglobulin; T_gAbon, antithyroglobulin antibody before Levothyroxine withdrawal; TSH_{off}, thyroid-stimulating hormone after Levothyroxine withdrawal; T_goff, stimulated thyroglobulin; T_gAboff, antithyroglobulin antibody after Levothyroxine withdrawal; IQR, interquartile range; RAIU, radioiodine uptake.

Variables displayed minimal multicollinearity, as indicated in **Figure 2a**. After screening and LASSO processing, key features distinguishing patients with and without ER included sex, TNM-N, risk stratification, RAIU%, T_gon, TSH_{off}, T_goff, and the count of previous 131I courses. These emerged as top indicators for the risk of non-ER, depicted in **Figures 2b and 2c**.

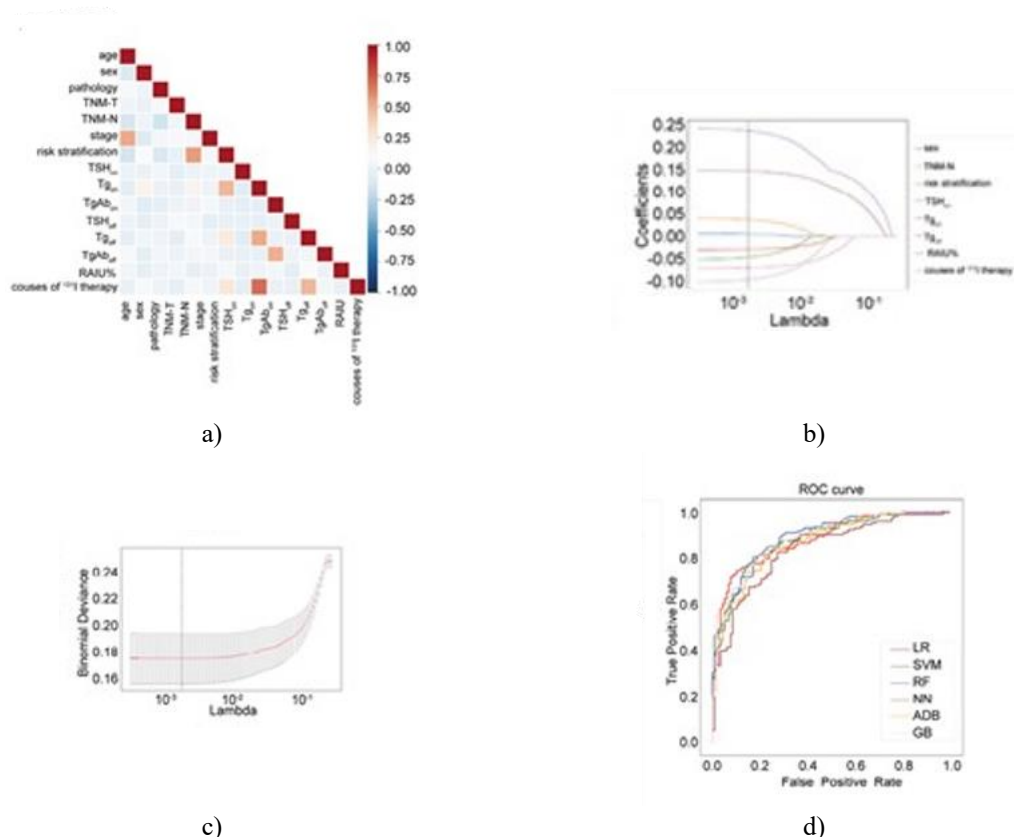


Figure 2. Development and validation of a machine learning model to predict treatment response to radioiodine (131I) therapy in patients with differentiated thyroid cancer without structural disease. (a) Correlation analysis among the factors included in the study that are linked to 131I therapy. (b) Application of the least absolute shrinkage and selection operator (LASSO) to identify the most influential factors associated with treatment response to 131I therapy. (c) Determination of the optimal λ corresponding to the lowest mean square error for selecting features. (d) Receiver operating characteristic curve (ROC) analysis showing the area under the curve (AUC) for predicting treatment response.

During model training, LG, SVM, RF, NN, ADA, and GB algorithms were employed, and their predictive performance was evaluated using AUC in the testing cohort. The findings indicated that all algorithms achieved similar predictive capabilities for treatment response to 131I therapy, with RF showing the highest accuracy of 81.3% and an AUC of 0.896, as presented in **Figure 2d**.

The impact of each influential factor within RF was assessed using SHAP analysis, shown in **Figure 3a**. Higher values of TNM-N, risk stratification, Tgon, and Tgoff prior to the current course of 131I therapy were linked to non-ER outcomes. Among these, Tgon and Tgoff before the current course emerged as the top two factors with the greatest influence on RF's prediction of 131I therapy response, as illustrated in **Figure 3b**. Furthermore, 10 RF ensembles, each containing 500 trees, were trained using the identified influential factors. The selection frequency of each factor at the root and at levels one to three of the trees in the ensembles was calculated to determine their relative importance. Node-splitting cutoff thresholds were chosen to maximize impurity reduction across all candidate splits [20]. One example of an RF ensemble is shown in **Figure 3c**. Predictions for a random sample of patients indicated ER to 131I therapy using this RF ensemble, as presented in **Figure 5d**. These predictions were consistent with final follow-up results, confirming the model's ability to accurately predict treatment response to 131I therapy.

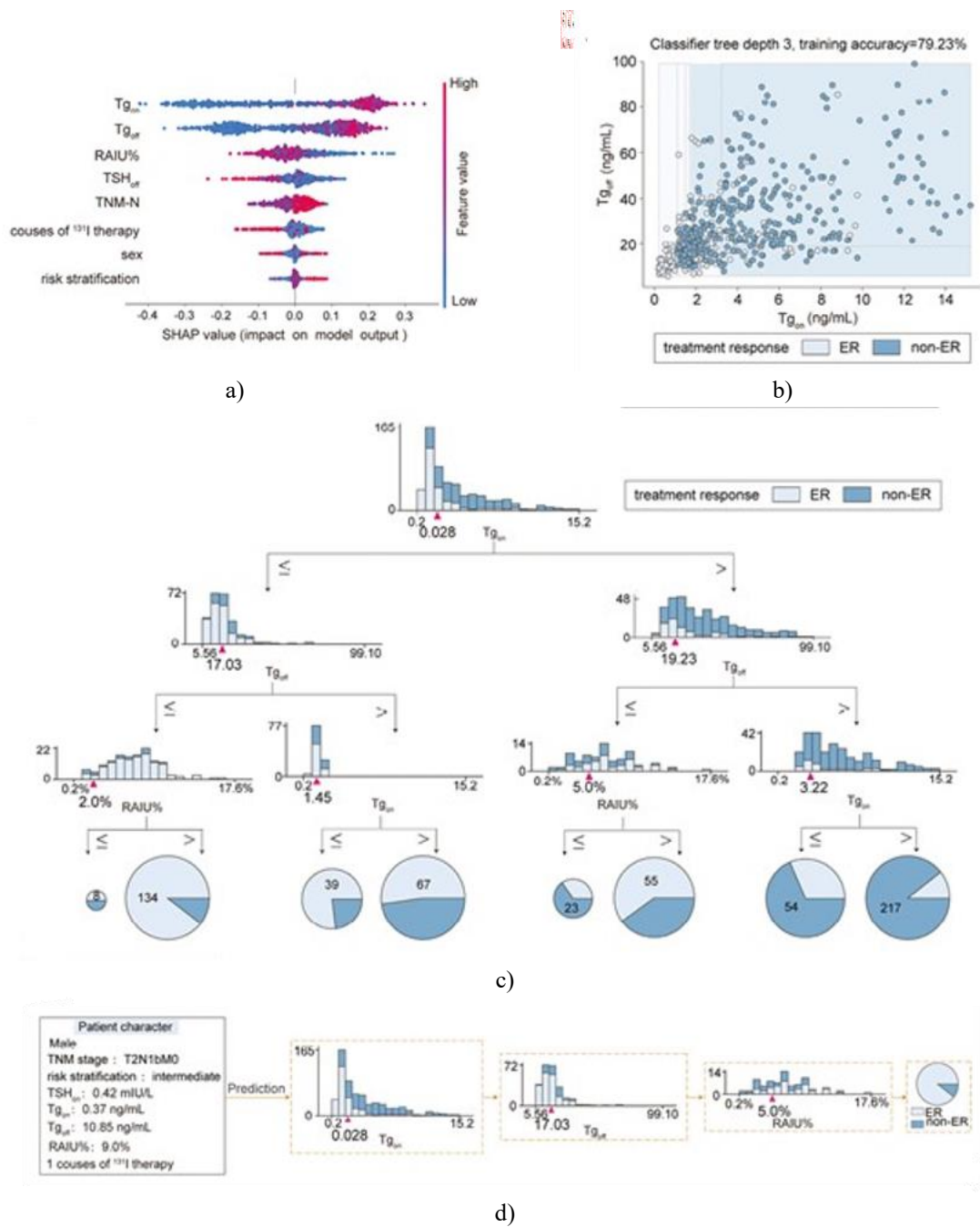


Figure 3. Random forest (RF) setup to forecast radioiodine (131I) outcomes among differentiated thyroid cancer cases lacking visible lesions. (a) SHAP overview of top variables' effects. (b) Linkage of off/on thyroglobulin states within RF framework. (c) Example tree cluster from RF aimed at 131I outcome calls. (d) Case study: RF applied to one patient's 131I response forecast.

Baseline data for TSH suppression outcome forecasts

Four to six months after final 131I ablation, Tg_{on} exceeded 0.2 ng/mL in 54.6% (326/597) training cases and 54.8% (141/257) validation cases. **Table 3** lists traits for TSH suppression modeling groups; only prior 131I rounds varied notably between sets.

Table 3. Core traits among differentiated thyroid cancer cases without lesions in training/validation groups for TSH suppression response modeling (N = 467).

Characteristic	Testing cohort (n = 141)	Training cohort (n = 326)	P-value
Sex		.75	

Female	92 (65.2%)	218 (66.9%)	
Male	49 (34.8%)	108 (33.1%)	
Age, median (years)	45 (IQR, 35–54)	43 (IQR, 35–53)	.41
Pathology		.18	
PTC	136 (96.5%)	321 (98.5%)	
FTC	5 (3.5%)	5 (1.5%)	
Tumor		.55	
T1	95 (67.4%)	208 (63.8%)	
T2	21 (14.9%)	65 (19.9%)	
T3	18 (12.8%)	34 (10.4%)	
T4	7 (4.9%)	19 (5.8%)	
Lymph node		.76	
N0	8 (5.7%)	22 (6.7%)	
N1a	44 (31.2%)	111 (34.0%)	
N1b	89 (63.1%)	193 (59.3%)	
Stage		.79	
I	114 (80.9%)	260 (79.8%)	
II	27 (19.1%)	63 (19.3%)	
III	0 (0%)	3 (0.9%)	
IV	0 (0%)	0 (0%)	
Risk stratification		.90	
Low	11 (7.8%)	22 (6.7%)	
Mediate	111 (78.7%)	258 (79.1%)	
High	19 (13.5%)	46 (14.1%)	
RAIU%, median	6.0 (IQR, 3.7–8.5)	6.1 (IQR, 3.5–8.5)	.80
Courses of 131I therapy		.08	
1	91 (64.5%)	181 (55.5%)	
>1	50 (35.5%)	145 (44.5%)	
TSHsix, median (mIU/L)	0.08 (IQR, 0.06–0.23)	0.12 (IQR, 0.06–0.27)	.46
Tgsix, median (ng/mL)	0.79 (IQR, 0.45–1.86)	1.08 (IQR, 0.51–1.97)	.16
TgAbsix, median (IU/mL)	12.00 (IQR, 10.00–18.00)	12.85 (IQR, 10.00–21.00)	.45
Thyroid remnant on Rx-WBS of the last course of therapy		.24	
Yes	42 (29.8%)	117 (35.9%)	
No	99 (70.2%)	209 (64.1%)	

Key terms: TSH, thyroid-stimulating hormone; PTC, papillary thyroid cancer; FTC, follicular thyroid cancer; RAIU, radioiodine uptake; TSHsix, thyroid-stimulating hormone at 4–6 months after the last course of 131I therapy; Tgsix, stimulated thyroglobulin at 4–6 months after the last course of 131I therapy; IQR, interquartile range; Rx-WBS, post-therapeutic whole-body scan.

Table 4. Trait contrasts for differentiated thyroid cancer cases without lesions achieving BR versus non-BR under TSH suppression across training/validation groups (N = 467).

Characteristic	Testing cohort (n = 141)		P-value	Training cohort (n = 326)		P-value
	BR (n = 72)	Non-BR (n = 69)		BR (n = 155)	Non-BR (n = 171)	
Sex	.01		.01			
Female	60 (83.3%)	32 (46.4%)		121 (78.1%)	97 (56.7%)	
Male	12 (16.7%)	37 (53.6%)		34 (21.9%)	74 (43.3%)	
Age, median (years)	46 (IQR, 38–55)	42 (IQR, 35–54)	.16	45 (IQR, 35–54)	43 (IQR, 34–53)	.38

Pathology	1.00		1.00			
PTC	69 (95.8%)	67 (97.1%)	153 (98.7%)	168 (98.2%)		
FTC	3 (4.2%)	2 (2.9%)	2 (1.3%)	3 (1.8%)		
Tumor stage	.49		.88			
T1	45 (62.5%)	50 (72.5%)	96 (61.9%)	112 (65.5%)		
T2	11 (15.3%)	10 (14.5%)	32 (20.7%)	33 (19.3%)		
T3	12 (16.7%)	6 (8.7%)	18 (11.6%)	16 (9.4%)		
T4	4 (5.5%)	3 (4.3%)	9 (5.8%)	10 (5.8%)		
Lymph node status	.01		.22			
N0	8 (11.1%)	0 (0%)	9 (5.8%)	13 (7.6%)		
N1a	26 (36.1%)	18 (26.1%)	60 (38.7%)	51 (29.8%)		
N1b	38 (52.8%)	51 (73.9%)	86 (55.5%)	107 (62.6%)		
Overall stage	.83		.52			
I	59 (81.9%)	55 (79.7%)	120 (77.4%)	140 (81.9%)		
II	13 (18.1%)	14 (20.3%)	33 (21.3%)	30 (17.5%)		
III	0 (0%)	0 (0%)	2 (1.3%)	1 (0.6%)		
IV	0 (0%)	0 (0%)	0 (0%)	0 (0%)		
Risk group	.01		.01			
Low	10 (13.8%)	1 (1.4%)	10 (6.5%)	12 (7.0%)		
Intermediate	57 (79.2%)	54 (78.3%)	133 (85.8%)	125 (73.1%)		
High	5 (7.0%)	14 (20.3%)	12 (7.7%)	34 (19.9%)		
RAIU%, median	5.5 (IQR, 3.7–8.6)	6.2 (IQR, 3.7–8.4)	.88	6.0 (IQR, 4.0–8.3)	6.2 (IQR, 3.2–8.9)	.78
Number of 131I therapy courses				.01		
1 course	58 (80.6%)	33 (47.8%)	115 (74.2%)	66 (38.6%)		
>1 course	14 (19.4%)	36 (52.2%)	40 (25.8%)	105 (61.4%)		
TSHsix, median (mIU/L)	0.13 (IQR, 0.07–0.33)	0.08 (IQR, 0.06–0.163)	.03	0.15 (IQR, 0.06–0.4)	0.08 (IQR, 0.06–0.21)	.01
Tgsix, median (ng/mL)	0.36 (IQR, 0.35–1.07)	1.47 (IQR, 0.62–3.57)	.01	0.65 (IQR, 0.38–1.34)	1.65 (IQR, 0.76–2.65)	.01
TgAbsix, median (IU/mL)	12.25 (IQR, 10.00–20.33)	12.00 (IQR, 10.00–18.00)	.71	14.00 (IQR, 10.00–23.00)	12.00 (IQR, 10.00–16.80)	.36
Thyroid remnant on Rx-WBS in last 131I course	.01		.01			
Yes	58 (80.6%)	33 (47.8%)	16 (10.3%)	101 (59.1%)		
No	14 (19.4%)	36 (52.2%)	139 (89.7%)	70 (40.9%)		

Key terms: TSH, thyroid-stimulating hormone; BR, biochemical remission; PTC, papillary thyroid cancer; FTC, follicular thyroid cancer; RAIU, radioiodine uptake; TSHsix, thyroid-stimulating hormone at 4–6 months after the last course of 131I therapy; Tgsix, stimulated thyroglobulin at 4–6 months after the last course of 131I therapy; TgAbsix, antithyroglobulin antibody at 4–6 months after the last course of 131I therapy; IQR, interquartile range; Rx-WBS, post-therapeutic whole-body scan.

Forecasting TSH suppression outcomes

Table 4 reports $\Delta\text{Tg}\text{on}\%$ shifts spanning 6 to 12–24 months post-final 131I: training saw 47.5% (155/326) hit BR thresholds against 52.5% (171/326) non-BR, while validation logged 51.1% (72/141) BR and 48.9% (69/141) non-BR.

Factors showed weak interlinks (**Figure 4a**). Univariate checks flagged sex, risk group, pre-final-131I RAIU%, TSHsix, Tgsix, 131I round totals, plus remnant uptake on last Rx-WBS as BR differentiators. Cross-validated LASSO pruned to sex, risk group, TSHsix, Tgsix, 131I totals, and last Rx-WBS remnant as prime non-BR signals (**Figures 4b–4c**).

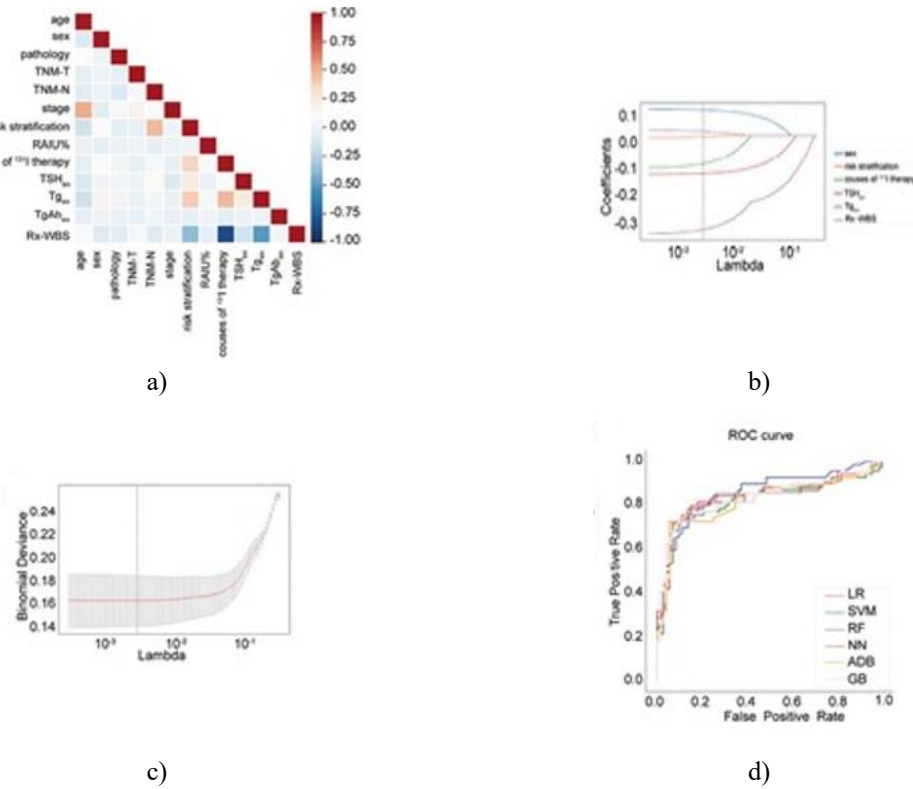
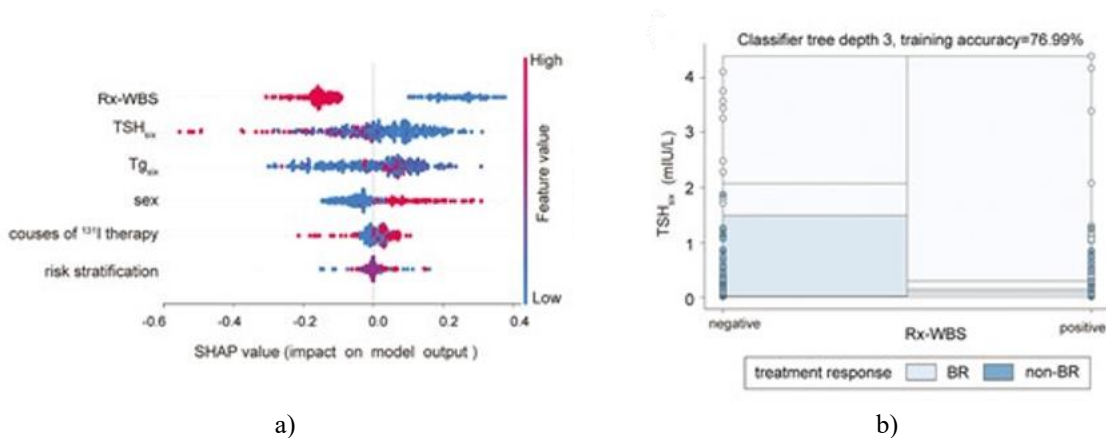


Figure 4. Machine learning pipeline build/test for thyrotropin (TSH) suppression response in differentiated thyroid cancer without lesions. (a) Variable interlinks tied to TSH suppression. (b) LASSO tuning of top response drivers for TSH suppression. (c) λ sweet spot minimizing error in feature picks. (D) ROC-AUC plot for TSH suppression response forecasts.

Training deployed LG, SVM, RF, NN, ADA, GB constructs, scored via test-set AUCs. RF topped charts at 78.7% accuracy, 0.857 AUC (Figure 4d).

Figure 5a displays the impact of key variables on the Random Forest model via SHAP interpretation. Presence of thyroid remnant on the post-therapy whole-body scan from the final 131I cycle, along with elevated TSH_{6x} values, showed a strong positive link to achieving BR under TSH suppression therapy. These two elements ranked as the top contributors driving RF forecasts for TSH suppression outcomes, as depicted in **Figure 5b**. An illustrative tree from one RF ensemble appears in **Figure 5c**. Application of this ensemble to a randomly chosen case correctly forecasted BR for TSH suppression therapy, presented in **Figure 5d**. The forecast aligned precisely with long-term clinical results, confirming the model's robustness for anticipating TSH suppression response.



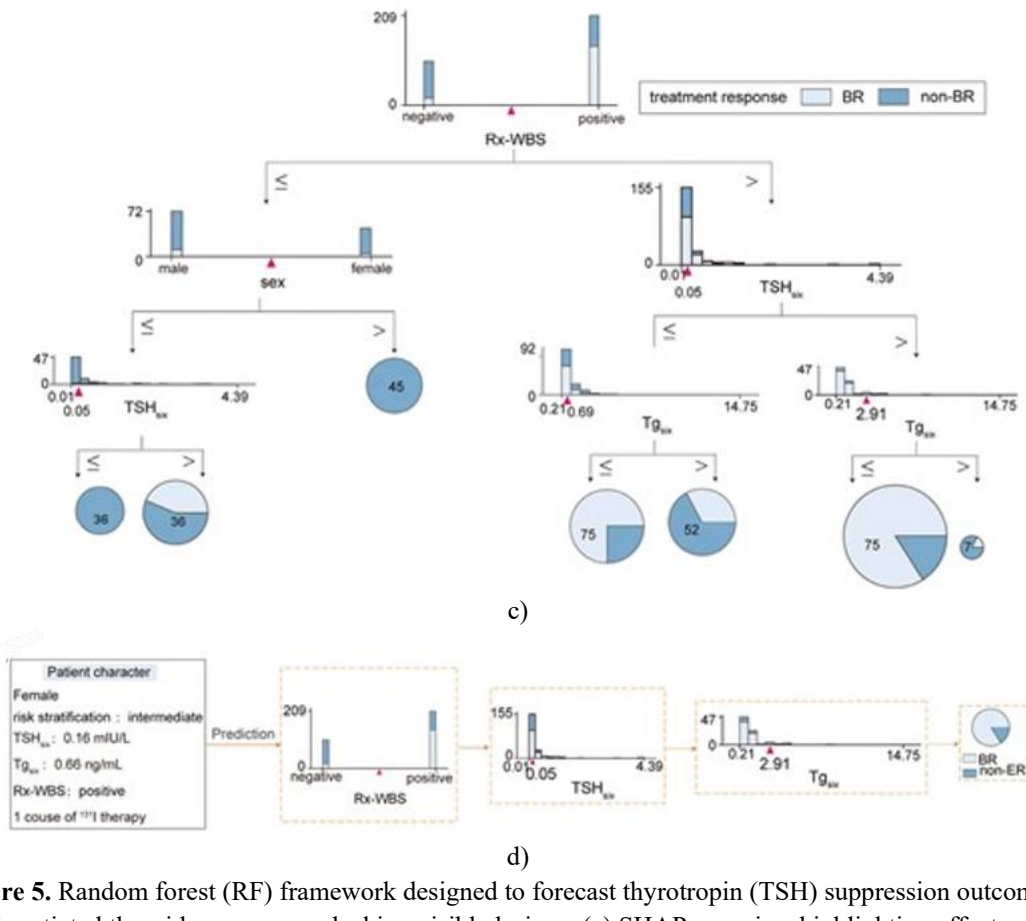


Figure 5. Random forest (RF) framework designed to forecast thyrotropin (TSH) suppression outcomes in differentiated thyroid cancer cases lacking visible lesions. (a) SHAP overview highlighting effects of top variables. (b) Relationship of TSH levels and remnant thyroid visibility on post-therapy scans within RF. (c) Sample tree structure from RF ensemble targeting TSH suppression response calls. (d) Example case: RF deployment for one patient's TSH suppression outcome projection.

As far as we are aware, this represents the initial effort to create machine learning systems capable of forecasting responses to both ¹³¹I therapy and TSH suppression therapy. Multiple predictive frameworks were developed to identify individuals likely to gain from these interventions, relying solely on baseline clinical data and laboratory indicators across a substantial patient group. Random Forest emerged as the superior performer. The resulting tools delivered strong classification precision for ER under ¹³¹I therapy and BR under TSH suppression, offering valuable support for clinical decision-making.

Clinical application of ¹³¹I therapy spans eight decades [21]. Historically, treatment protocols have drawn on elements like surgical pathology details, radioiodine imaging findings, plus TSH and Tg measurements [22, 23]. In the current analysis, predictors of ¹³¹I response included sex, risk category, TNM-N stage, RAIU%, Tgon, Tgoff, TSHoff, and prior ¹³¹I cycle count. Males exhibited superior Tg reduction, aligning with earlier reports linking elevated estrogen to increased Tg expression—possibly through enhanced release of mutagenic agents in thyroid tissue and promotion of tumor growth [24]. Risk stratification displayed a modest inverse tie with ER likelihood; while ¹³¹I is typically advised for higher-risk cases [25], such patients proved harder to reach ER, implying need for alternative approaches to Tg control. Residual thyroid tissue remains the primary driver of persistent high Tg post-thyroidectomy. Pre-therapy RAIU% assesses remnant activity [26], and detectable pre-cycle Tg signals ongoing remnant or biochemical persistence, aiding therapy planning [12]. Prior work by Li *et al.* tied Tgoff closely to ER after first ¹³¹I administration, identifying a cutoff of 6.915 µg/L yielding 69.2% sensitivity and 89.4% specificity [27]. Our results similarly underscored major roles for RAIU% and Tg in ER projection. Most cases retained ¹³¹I uptake in the thyroid bed or thyroglossal remnants on post-therapy scans, particularly post-initial cycle. Tg declines grew evident with additional cycles, supporting the value of repeat ¹³¹I administrations for response attainment.

Cases showing elevated Tg alongside negative Rx-WBS often warrant further investigation and potential adjunct interventions [3, 12, 28]. Notably, among those with non-avid lesions post-current cycle, Tgon fell below 0.2 ng/mL after extra 131I rounds in 26.3% (49/186) training cases and 26.6% (21/79) testing cases. This reinforces high Tg as a marker prompting adjuvant measures to lower levels and streamline staging plus monitoring [28, 29].

TSH suppression therapy serves as a key strategy following thyroidectomy and 131I treatment in thyroid cancer management. It inhibits thyroid cancer cell proliferation and promotes Tg reduction by keeping TSH below normal ranges [30]. Among the variables examined here, our work provides the first robust evidence that visible thyroid remnant on the post-therapy whole-body scan from the final 131I cycle, combined with elevated TSHsix, reliably marks patients likely to gain biochemical remission from TSH suppression. Raised TSHsix typically signals inadequate levothyroxine dosing; with proper adjustment, Tg usually drops quickly. Individuals classified as intermediate- or high-risk DTC may derive limited advantage from this approach [31]. Remnant thyroid tissue detected on the last Rx-WBS often explains persistent Tg elevation. To minimize any lingering influence from prior 131I on Tg values, response evaluation compared Tgon at 6 months versus 12-24 months after the final 131I administration. Still, residual 131I effects at the 6-month mark cannot be fully excluded. Furthermore, nadir Tg achievement rates rise gradually during ongoing suppression, supporting a conservative stance—avoiding extra interventions in cases with stably low Tg and no structural lesions [32]. We noted Tg reductions mainly among those starting with modest elevations. Yet nearly half the cohort with higher baseline Tg failed to show decline. Potential reasons include suboptimal medication compliance or issues affecting drug absorption/metabolism [33]. Alternatively, prior 131I cycles might have lacked efficacy, especially in aggressive or advanced cases where ablation proves incomplete. Rising Tg can also signal early recurrence, warranting additional diagnostics. Certain basic traits, like sex, correlate with spontaneous Tg fall but fall outside ATA risk frameworks. Consistent with 131I findings, males responded better to suppression. Nonetheless, therapy choices must remain tailored, balancing risks against expected gains for every individual.

Here, we integrated selected predictors into six machine-learning frameworks—Logistic Regression (LR), Support Vector Classifier (SVC), Random Forest (RF), Neural Network (NN), Adaptive Boosting (ADA), and Gradient Boosting (GB)—to forecast responses to 131I or TSH suppression. All approaches performed similarly, though RF achieved top accuracy and AUC values. RF operates as an ensemble method, constructing numerous decision trees via bagging and random feature selection. Each tree trains on distinct data subsets using varied feature combinations, then aggregates outputs for the final call. This randomness enhances robustness, curbs overfitting, and allows capture of intricate feature-outcome interactions, driving superior precision [34, 35]. By incorporating routine pre-intervention clinical and laboratory data, RF effectively separates likely beneficiaries from non-responders ahead of treatment.

Certain constraints apply to this work. First, the retrospective design focused on DTC cases without structural disease who underwent at least one 131I cycle, potentially introducing selection bias and limiting generalizability to untreated cohorts at our center. Second, recruitment occurred at one facility; validation across external sites would strengthen conclusions. Third, predictors relied solely on available pre-treatment clinical and biochemical elements. Key potential influencers, such as BRAF mutation status, were omitted owing to extensive missing records.

Conclusion

These results establish machine-learning approaches, particularly Random Forest, as powerful instruments for anticipating responses to 131I therapy and TSH suppression therapy among differentiated thyroid cancer patients lacking structural disease, using only standard pre-treatment clinical parameters and laboratory indicators.

Acknowledgments: None

Conflict of Interest: None

Financial Support: None

Ethics Statement: None

References

1. Kitahara CM, Sosa JA. The changing incidence of thyroid cancer. *Nat Rev Endocrinol*. 2016;12(11):646–53. doi:10.1038/nrendo.2016.110
2. Van Den Heede K, Tolley NS, Di Marco AN, Palazzo FF. Differentiated thyroid cancer: A health economic review. *Cancers* 2021;13(9):2253. doi:10.3390/cancers13092253
3. Haugen BR, Alexander EK, Bible KC, et al. 2015 American thyroid association management guidelines for adult patients with thyroid nodules and differentiated thyroid cancer: The american thyroid association guidelines task force on thyroid nodules and differentiated thyroid cancer. *Thyroid* 2016;26(1):1–133. doi:10.1089/thy.2015.0020
4. Klain M, Nappi C, Zampella E, et al. Ablation rate after radioactive iodine therapy in patients with differentiated thyroid cancer at intermediate or high risk of recurrence: A systematic review and a meta-analysis. *Eur J Nucl Med Mol Imaging*. 2021;48(13):4437–44. doi:10.1007/s00259-021-05440-x
5. Gluvic Z, Obradovic M, Stewart AJ, et al. Levothyroxine treatment and the risk of cardiac arrhythmias - focus on the patient submitted to thyroid surgery. *Front Endocrinol*. 2021;12:758043. doi:10.3389/fendo.2021.758043
6. Biondi B, Cooper DS. Thyroid hormone suppression therapy. *Endocrinol Metab Clin North Am*. 2019;48(1):227–37. doi:10.1016/j.ecl.2018.10.008
7. Cheng X, Xu S, Zhu Y, et al. Markedly elevated serum preoperative thyroglobulin predicts radioiodine-refractory thyroid cancer. *Eur J Clin Invest*. 2022;52(4):e13721. doi:10.1111/eci.13721
8. Francis Z, Schlumberger M. Serum thyroglobulin determination in thyroid cancer patients. *Best Pract Res Clin Endocrinol Metab* 2008;22(6):1039–46. doi:10.1016/j.beem.2008.09.015
9. Zöphel K, Wunderlich G, Kotzerke J. A highly sensitive thyroglobulin assay has superior diagnostic sensitivity for recurrence of differentiated thyroid cancer in patients undergoing TSH suppression. *J Nucl Med* 2006;47(3):552–3.
10. Evans C, Tennant S, Perros P. Thyroglobulin in differentiated thyroid cancer. *Clin Chim Acta* 2015;444:310–17. doi:10.1016/j.cca.2014.10.035
11. Hu HY, Liang J, Zhang T, Zhao T, Lin Y-S. Suppressed thyroglobulin performs better than stimulated thyroglobulin in defining an excellent response in patients with differentiated thyroid cancer. *Nucl Med Commun*. 2018;39(3):247–51. doi:10.1097/MNM.0000000000000796
12. Cheng L, Sa R, Luo Q, et al. Unexplained hyperthyroglobulinemia in differentiated thyroid cancer patients as an indication for radioiodine adjuvant therapy: A prospective multicenter study. *J Nucl Med* 2021;62(1):62–8. doi:10.2967/jnumed.120.243642
13. Klain M, Zampella E, Piscopo L, et al. Long-term prognostic value of the response to therapy assessed by laboratory and imaging findings in patients with differentiated thyroid cancer. *Cancers* 2021;13(17):4338. doi:10.3390/cancers13174338
14. Ma C, Xie J, Kuang A. Is empiric 131i therapy justified for patients with positive thyroglobulin and negative 131i whole-body scanning results?. *J Nucl Med* 2005;46(7):1164–70.
15. Wang PW, Wang ST, Liu RT, et al. Levothyroxine suppression of thyroglobulin in patients with differentiated thyroid carcinoma. *J Clin Endocrinol Metab*. 1999;84(12):4549–53. doi:10.1210/jcem.84.12.6190
16. Leboulleux S, Bournaud C, Chouquet CN, et al. Thyroidectomy without radioiodine in patients with low-risk thyroid cancer. *N Engl J Med*. 2022;386(10):923–32. doi:10.1056/NEJMoa2111953
17. Verburg FA, Flux G, Giovannella L, et al. Differentiated thyroid cancer patients potentially benefitting from postoperative i-131 therapy: A review of the literature of the past decade. *Eur J Nucl Med Mol Imaging*. 2020;47(1):78–83. doi:10.1007/s00259-019-04479-1
18. Kawakami E, Tabata J, Yanaihara N, et al. Application of artificial intelligence for preoperative diagnostic and prognostic prediction in epithelial ovarian cancer based on blood biomarkers. *Clin Cancer Res* 2019;25(10):3006–15. doi:10.1158/1078-0432.CCR-18-3378
19. Cruz JA, Wishart DS. Applications of machine learning in cancer prediction and prognosis. *Cancer Inf*. 2007;2:59–77.
20. Luna JM, Chao HH, Diffenderfer ES, et al. Predicting radiation pneumonitis in locally advanced stage II-III non-small cell lung cancer using machine learning. *Radiother Oncol*. 2019;133:106–12.

doi:10.1016/j.radonc.2019.01.003

21. Jhiang SM, Sipos JA. Na⁺/I⁻ symporter expression, function, and regulation in non-thyroidal tissues and impact on thyroid cancer therapy. *Endocr Relat Cancer*. 2021;28(10):T167–T177. doi:10.1530/ERC-21-0035
22. Avram AM, Zukotynski K, Nadel HR, Giovanella L. Management of differentiated thyroid cancer: The standard of care. *J Nucl Medicine* 2022;63(2):189–95. doi:10.2967/jnumed.121.262402
23. Zheng W, Rui Z, Wang X, et al. The influences of tsh stimulation level, stimulated tg level and tg/tsh ratio on the therapeutic effect of (131)i treatment in dtc patients. *Front Endocrinol*. 2021;12:601960. doi:10.3389/fendo.2021.601960
24. Shobab L, Burman KD, Wartofsky L. Sex differences in differentiated thyroid cancer. *Thyroid* 2022;32(3):224–35. doi:10.1089/thy.2021.0361
25. Avram AM. Radioiodine scintigraphy with spect/ct: An important diagnostic tool for thyroid cancer staging and risk stratification. *J Nucl Med* 2012;53(5):754–64. doi:10.2967/jnumed.111.104133
26. Jin Y, Ruan M, Cheng L, et al. Radioiodine uptake and thyroglobulin-guided radioiodine remnant ablation in patients with differentiated thyroid cancer: A prospective, randomized, open-label, controlled trial. *Thyroid* 2019;29(1):101–10. doi:10.1089/thy.2018.0028
27. Li Y, Rao M, Zheng C, et al. Analysis of factors influencing the clinical outcome after surgery and (131)i therapy in patients with moderate-risk thyroid papillary carcinoma. *Front Endocrinol*. 2022;13:1015798. doi:10.3389/fendo.2022.1015798
28. Tuttle RM, Ahuja S, Avram AM, et al. Controversies, consensus, and collaboration in the use of (131)i therapy in differentiated thyroid cancer: A joint statement from the american thyroid association, the european association of nuclear medicine, the society of nuclear medicine and molecular imaging, and the european thyroid association. *Thyroid* 2019;29:461–70.
29. Sun YQ, Sun D, Zhang X, Zhang Y-Q, Lin Y-S. Radioiodine adjuvant therapy in differentiated thyroid cancer: An update and reconsideration. *Front Endocrinol*. 2022;13:994288. doi:10.3389/fendo.2022.994288
30. Bruno R, Ferretti E, Tosi E, et al. Modulation of thyroid-specific gene expression in normal and nodular human thyroid tissues from adults: An in vivo effect of thyrotropin. *J Clin Endocrinol Metab*. 2005;90(10):5692–7. doi:10.1210/jc.2005-0800
31. Klubo-Gwiezdzinska J, Auh S, Gershengorn M, et al. Association of thyrotropin suppression with survival outcomes in patients with intermediate- and high-risk differentiated thyroid cancer. *JAMA Netw Open* 2019;2(2):e187754. doi:10.1001/jamanetworkopen.2018.7754
32. Padovani RP, Robenshtok E, Brokhin M, Tuttle RM. Even without additional therapy, serum thyroglobulin concentrations often decline for years after total thyroidectomy and radioactive remnant ablation in patients with differentiated thyroid cancer. *Thyroid* 2012;22(8):778–83. doi:10.1089/thy.2011.0522
33. Alkaf B, Siddiqui M, Ali T, et al. Ramadan fasting and changes in thyroid function in hypothyroidism: Identifying patients at risk. *Thyroid* 2022;32(4):368–75. doi:10.1089/thy.2021.0512
34. Ganaie MA, Tanveer M, Suganthan PN, Snasel V. Oblique and rotation double random forest. *Neural Netw* 2022;153:496–517. doi:10.1016/j.neunet.2022.06.012
35. Nakayama JY, Ho J, Cartwright E, Simpson R, Hertzberg VS. Predictors of progression through the cascade of care to a cure for hepatitis c patients using decision trees and random forests. *Comput Biol Med*. 2021;134:104461. doi:10.1016/j.combiomed.2021.104461